Opt Quant Electron (2012) 44:45–54
DOI 10.1007/s11082-011-9531-2

Analysis and improvement of optical frequency response in a long wavelength transistor laser

Hassan Rahbardar Mojaver · Hassan Kaatuzian

Received: 27 September 2011 / Accepted: 16 December 2011 / Published online: 29 December 2011

Abstract Charge control model and rate equations have been exploited for the first time in order to glean the optical frequency response of a long-wavelength heterojunction bipolar transistor laser. For a 1.56 µm N-InP/p-InAlGaAs/N-InP fabricated transistor laser with a single quantum well, the optical bandwidth is estimated using this model. All parameters of the mentioned model have been computed for this new type of long wavelength transistor laser. It has been found that frequency response of this optoelectronic device has a 29 dB resonance peak which is not very desirable and is so higher than traditional GaAs transistor lasers. Furthermore, we have illustrated that the resonance peak will decrease and the optical bandwidth will increase, if we increase the width of the quantum well. Finally, we have analyzed that how base width affects on the optical bandwidth and resonance peak of frequency response. It has been proved that, there is a trade-off between larger bandwidth and lower resonance peak for base width effect.

Keywords Transistor laser · Long-wavelength · Optical frequency response · Quantum well · Base width effect

1 Introduction

The invention of Transistor Lasers (TL) in year 2006, made it possible, the creation of an electronic device which works as transistor and laser with two optical and electrical outputs simultaneously (Holonyak and Feng 2006; Kaatuzian 2005). This device is a Heterojunction Bipolar Transistor (HBT) with a Quantum Well (QW) in its base, which reduce carrier life time in the base region, and increase photon generation subsequently. The first generation of

H. R. Mojaver (✉) · H. Kaatuzian
Electrical Engineering Department, Photonic Research Laboratory (PRL),
Amirkabir University of Technology, Hafez Avenue #424, 15914 Tehran, Iran
e-mail: kaveh.rahbardar@aut.ac.ir

H. Kaatuzian
e-mail: hsnkato@aut.ac.ir

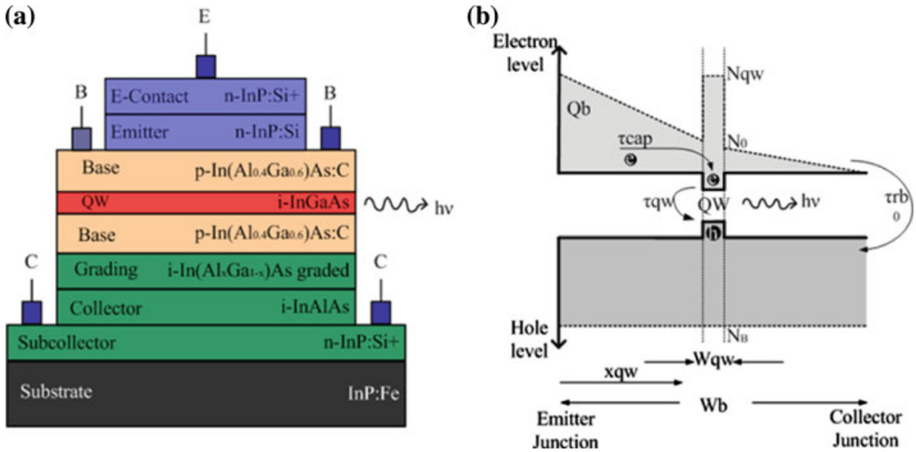

Fig. 1 **a** The epitaxial structure of the long wavelength TL, **b** charge control model for the TL under base-emitter forward bias and base-collector reverse bias. The electron recombination and photon generation inside the QW are illustrated

TLs has been dominantly fabricated from GaAs-based materials, and thereby the emission wavelength is limited to near-infrared region ($\lambda \sim 1\,\mu$m) (Feng and Holonyak 2005). For fiber optical communication applications, the operating wavelength should be extended to either 1.3 or 1.55 μm. So the InP-based materials TLs such as InAlGaAs/InP have been introduced (Dixon et al. 2008; Huang and Ryou 2011).

Figure 1a shows the epitaxial structure of the N-InP/p-$In_{0.53}(Al_{0.4}Ga_{0.6})_{0.47}As$/N-InP transistor laser with the emission wavelength of 1.56 μm which is analyzed in this work. In this structure the InP emitter and collector serve as the cladding layers and $In_{0.53}(Al_{0.4}Ga_{0.6})_{0.47}As$ base serves as the waveguide layer. An 8 nm undoped $In_{0.58}Ga_{0.42}As$ QW is placed in the middle of base too. Experimentally Hung et al. have demonstrated a TL based on this structure operating at 77 K in continues-wave mode (Huang and Ryou 2011; Huang et al. 2011).

Previous works for traditional GaAs TLs show that, optimizing various parameters of TLs like base width, QW width and QW location, will improve TLs characteristics like optical frequency response (Kaatuzian et al. 2011; Taghavi and Kaatuzian 2010). In this work, we study QW and base width effect on optical frequency response of InP based material long-wavelength TLs using a charge control model, in order to improve their optical frequency response.

2 Modeling

For obtaining the frequency response of transistor lasers, an appropriate model for transistor laser is needed. In this work coupled rate equations which are based on charge control model have been used (Zhang and Leburton 2009). Figure 1b shows the schematic of important processes in the base region of the sample HBTL, under active bias condition. In this figure the electrons diffuse across the base region from left side (Emitter junction) to the right side (Collector junction) and some of them recombine with the holes in this movement. The base width is shown by W_b when W_{qw} and x_{qw} are QW width and the distance of QW from emitter junction. The recombination occurs via two processes. The first one is the direct recombination outside the QW region with the life time of τ_{rb0} and the second one which is more possible is recombination inside the QW. For this type of recombination, the electrons are captured in the QW with the electron capture time of τ_{cap} and then recombine with the holes with recombination life time of τ_{qw}^{eff}. We consider a two-level system in which the electron and holes recombination only occurs between ground states, so it can be said that if the base current is below the threshold level $\tau_{qw}^{eff} = \tau_{qw}$, τ_{qw} is the lifetime via spontaneous emission which will be explained later. But when the base current is above the threshold level, since both spontaneous and stimulated emission occurs, τ_{qw}^{eff} will be calculated by Eq. (1).

$$\tau_{qw}^{eff} = \left(1/\tau_{qw} + 1/\tau_{st}\right)^{-1} \tag{1}$$

In which τ_{st} is recombination lifetime via stimulated emission and defines in this way:

$$\tau_{st} = \left[\Omega N_p(t)\right]^{-1} \tag{2}$$

In Eq. (2), Ω is differential gain factor which will be explained later and $N_p(t)$ is photon density. Now we can use coupled rate equations to describe the TL action:

$$\frac{dn(t)}{dt} = \frac{\upsilon Q_b(t)}{\tau_{cap}} - \frac{n(t)}{\tau_{qw}} - \Omega\left[n(t) - n_{tr}\right] N_p(t) \tag{3}$$

$$\frac{dN_p(t)}{dt} = \Omega\left[n(t) - n_{tr}\right] N_p(t) + \frac{\theta n(t)}{\tau_{qw}} - \frac{N_p(t)}{\tau_p} \tag{4}$$

$$\frac{dQ_b(t)}{dt} = \frac{J(t)}{q} - \frac{Q_b(t)}{\tau_{rb}} \tag{5}$$

$$\frac{1}{\tau_{rb}} = \frac{1-\upsilon}{\tau_{rb0}} + \frac{\upsilon}{\tau_{cap}} \tag{6}$$

Equations (3) and (4) are the coupled rate equations for electron-photon interaction in the QW. In these equation n(t) is electron density and $N_p(t)$ is photon density. In Eq. (3), ν is QW geometry factor which gives the fraction of base charges captured in the QW and defines by $\nu = (W_{qw}/W_b)(1 - x_{qw}/W_b)$. so, $\nu Q_b(t)/\tau_{cap}$ is the base charge captured in the QW. $n(t)/\tau_{qw}$ is electron spontaneous recombination rate inside the QW, $\Omega[n(t) - n_{tr}]\ N_p(t)$ is the stimulated emission rate and n_{tr} is the transparency electron density. This equation has formulated the rate of change in charges in terms of photon generation rate by stimulated and spontaneous recombination and charges captured in the QW. In Eq. (4), θ is fraction of spontaneous emission which is coupled to the cavity mode and $N_p(t)/\tau_p$ is photon loss. We can ignore the term $\theta n(t)/\tau_{qw}$ because in this work $\tau_{qw}/\theta \sim 10\,\text{ns}$, which is at least two order of magnitude larger than any other time scales. Rate of variation in photons has been expressed as a function of photon generation rate by stimulated and spontaneous recombination and the rate of photon loss in Eq. (4). In Eq. (5), J(t) is base current density, and $Q_b(t)/\tau_{rb}$ is the base charge loss in which $1/\tau_{rb}$ is base charge loss rate which is weighted sum of the loss rate caused by the recombination outside the QW and by the QW capture process and is mentioned in Eq. (6).

The steady state solution for electron and photon densities can be obtained by setting $dn(t)/dt = 0$, $dN_p/dt = 0$ and $dQ(t)/dt = 0$ in (3)–(5):

$$n_0 = n_{tr} + \frac{1}{\Omega\tau_p} \tag{7}$$

$$N_{p0} = n_0 \frac{\tau_p}{\tau_{qw}} \left(\frac{J_0}{J_{th}} - 1\right) \tag{8}$$

In which J_{th} is the threshold current density and define as:

$$J_{th} = \frac{qn_0 \tau_{cap}}{\upsilon \tau_{qw} \tau_{rb}} \tag{9}$$

Now, small signal analysis can be performed by superimposing a small sinusoidal signal to the dc value which means $J(t) = J_0 + \Delta J(t)$. By using phasor analysis, optical output $S(\omega)$ can be defined as:

$$S(\omega) = \frac{\Delta N_p(\omega)}{\Delta J(\omega)} \tag{10}$$

Solving Eq. (10) in phasor domain using Eq. (3)–(9) will result in:

$$S(\omega) = \left(\frac{1}{1 + i\omega\tau_{rb}}\right) \frac{A}{\omega_r^2 - \omega^2 + i\omega\gamma} \tag{11}$$

In which:

$$A = \frac{\Omega \upsilon N_{p0} \tau_{rb}}{q\tau_{cap}} \tag{12}$$

$$\omega_r^2 = \frac{\Omega N_{p0}}{\tau_p} \tag{13}$$

$$\gamma = \frac{1}{\tau_{qw}} + \Omega N_{p0} \tag{14}$$

3 Modeling parameters

By using Eq. (11) optical frequency response of a HBTL can be obtained, but first we should define the parameters and constants in this equation, especially for long wavelength HBTL which is used in this work. In this part we define the parameters and constants of the model which explained in previous part.

3.1 τ_{qw}

The emission of light by a charge carrier is essentially a scattering event between an initial state 'i' and a final state 'f'. The electromagnetic field is the time-dependent perturbation $\tilde{H}$ which induces this event. The transition rate from the initial electronic state to the final state is given by Fermi's Golden Rule (Harrison 2005):

$$\frac{1}{\tau_{qw}} = \frac{2\pi}{\hbar} \sum_f \left| \left\langle f|\tilde{H}|i \right\rangle \right|^2 \delta(E_f^c - E_i^c + \hbar\omega) \tag{15}$$

where the superscript on the energies has been introduced to indicate that, these are the total carrier energies, which contain both kinetic and potential energy components.

The actual lifetime for intersubband spontaneous radiative emission is obtained by summing Eq. (15) over all photon modes. Conveniently, Smet et al. quotes the results as (Smet et al. 1996):

$$\frac{1}{\tau_{qw}} = \frac{q^2\omega}{4\varepsilon m^* c^2 W_{qw}} O_{if} \tag{16}$$

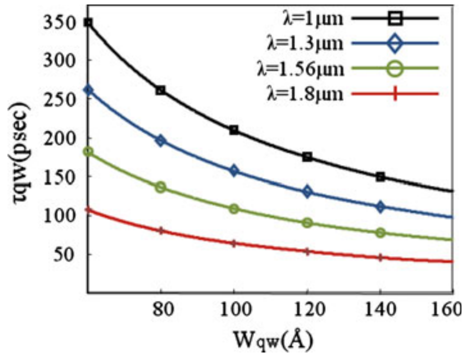

Fig. 2 Recombination lifetime via spontaneous emission, τ_{qw} versus W_{qw} for different wavelengths

where, O_{if} is oscillator strength which is dependent on the dipole matrix element by (Berger 1994):

$$O_{if} = \frac{2m^*\omega}{\hbar} |\langle\psi_i|z|\psi_f\rangle|^2 \tag{17}$$

where ω is angular frequency of light, and m^* is reduced effective mass given by $(m_e^* m_h^*)/(m_e^* + m_h^*)$, m_e^* and m_h^* are the effective masses of electrons and holes, respectively. Figure 2 shows τ_{qw} versus W_{qw} for different wavelengths which calculated by Eq. (15).

3.2 τ_{cap}

Electron capture time in quantum well (τ_{cap}) is the transit time of electron from emitter junction to QW. Since the diffusion constant assumed to be uniform throughout the base region, $D = 26\,cm^2\,s^{-1}$, we can write (Feng et al. 2007; Then et al. 2007):

$$\tau_{cap} = \frac{x_{qw}}{2D} \tag{18}$$

3.3 τ_{rb0}

Base charge bulk life time is the recombination life time of carriers in the base region except QW. It can be related to the quantity B_{rad}, the bimolecular radiative recombination coefficient by:

$$\tau_{rb0} = \frac{1}{B_{rad}N_B} \tag{19}$$

where, N_B is the hole density of base. The value of B_{rad} is reported to be $1.9 \times 10^{-10}\,cm^3\,s^{-1}$ for GaAs. (Then et al. 2007) Since Eq. (19) is an approximate equation we can assume the same value for InAlGaAs in this work with no remarkable error.

3.4 τ_p

The photon lifetime (τ_p) can be obtained from Eq. (20) in which L is the cavity length, R1, R2 are cavity facet reflectivity and n is refractive index. α_i is photon absorption which is obtained from Eq. (21) (Feng et al. 2006; Dixon et al. 2008):

$$\frac{1}{\tau_p} = \left(\frac{c}{n_r}\right)\left[\alpha_i + \frac{1}{2L}\ln\left(\frac{1}{R_1R_2}\right)\right] \tag{20}$$

$$\alpha_i = \left(\Gamma_{WG} + \Gamma_{QW}\right)k_pN_B \tag{21}$$

In which k_p is intervalence band absorption (Asada 1984), Γ_{WG} is the waveguide optical confinement factor and Γ_{QW} is quantum well optical confinement factor. It should be mentioned that the base region is the waveguide in this work.

3.5 Ω, n_{tr}

Stimulated recombination rate R_{st} is calculated by Eq. (22) in which g is the optical gain and derive from Eq. (23) (Coldren and Corzine 1995):

$$R_{st} = \frac{c}{n_r}gN_p \tag{22}$$

$$g = \frac{h\lambda^2m^*}{2n_r^2\tau_{qw}W_{qw}}\left(1 - e^{-N_{QW}/N_c} - e^{-N_B/N_V}\right) \tag{23}$$

$$N_{QW} = \frac{\tau_{esc}}{\tau_{cap}}N_0 \tag{24}$$

N_C and N_V are density of states of conduction and valance bands, and N_{QW} is Bounded carrier density in the QW, which is derived from Eq. (24) (Huang and Ryou 2011). In this equation τ_{esc} is the carrier thermionic escape lifetime which is normally one order of magnitude larger than τ_{qw}. (Faraji et al. 2009) and N_0 is the average unbounded carrier density around the QW which is set by boundary condition at the reverse-biased base-collector junction. N_0 and N_{QW} are also shown in Fig. 1b.

Equation (23) shows that g is a logarithmic function of N_B but since for many situations only small portion of the curve near and above the transparency point is of interest, a straight line approximation is often very useful, that is:

$$g = a(n - n_{tr}) \tag{25}$$

where a is the differential gain, dg/dn, and n_{tr} is the transparency carrier density. Using linear approximation of g in Eq. (22) leads to a linear approximation for stimulated emission which shows by $\Omega[n(t) - n_{tr}]N_p$ in Eqs. (3) and (4). From Eqs. (25), (22) it is clear that $\Omega = (c/n_r)^*a$. All of the modeling parameters which have been defined in this part are summarized in Table 1.

4 Results

In this part the optical frequency response of the TL will be obtained by placing the parameters which have been defined in part 3, in Eq. (11). The main physical parameters of the long wavelength TL which has been fabricated by Huang et al. and has been used in this work are summarized in Table 2 (Huang and Ryou 2011). Figure 3 shows the optical frequency response of this TL. The cutoff frequency of this TL is 12.3 GHz which is lower than GaAs TLs cutoff frequency. The cutoff frequencies of traditional GaAs TLs are more than 30 GHz (Feng et al. 2007). The other fact which is more important is the high resonance peak of the frequency response for this TL. The curve shows 29 dB peak which is not desirable and to some extent the low bandwidth is related to this fact. For GaAs TLs there is no resonance

Table 1 Modeling parameters for the transistor laser

Symbol	Definition	Unit
τ_{qw}	Recombination lifetime via spontaneous emission in QW	s
τ_{st}	Recombination lifetime via stimulated emission in QW	s
ν	Geometry factor	Unitless
τ_{cap}	Electron capture time in quantum well	s
τ_{rb}	Base charge life time	s
τ_{rb0}	Base charge bulk lifetime	s
τ_p	Photon lifetime	s
Ω	Differential gain factor	$m^2\ s^{-1}$
n_{tr}	Transparency electron density	m^{-2}

Table 2 Physical parameters of the long wavelength TL

Symbol	Definition	Value	Unit
W_b	Base width	108	nm
W_{qw}	Quantum well width	80	Å
x_{qw}	Distance from emitter junction to QW	500	Å
Λ	Wavelength	1.56	µm
T	Temperature	77	K
N_b	Base doping	1×10^{19}	cm^{-3}
n_r	Refractive index	3.34	Unitless
k_p	Intervalence band absorption	4×10^{-17}	cm^2
Γ_{WG}	Waveguide optical confinement factor	0.1	Unitless
Γ_{QW}	Quantum well optical confinement factor	0.01	Unitless
R_1, R_2	Facet reflectivity	0.3	Unitless
L	Cavity length	800	µm
D	Diffusion constant across base region	26	$cm^2\ s^{-1}$
N_c	Density of states of conduction bands	7×10^{17}	cm^{-3}
N_v	Density of states of valance bands	3×10^{18}	cm^{-3}

peak while for diode laser this resonance peak is in the order of 5 dB. The most important reason of this high resonance peak is low differential gain factor (Ω) for the new material which equals to $9.7 \times 10^{-3}\ cm^2\ s^{-1}$ as we calculated, while this parameter was $0.5\ cm^2\ s^{-1}$ for GaAs TLs (Zhang and Leburton 2009).

The other curves in Fig. 3 show that, increasing the QW width will result in decreasing the resonance peak and improvement of optical frequency response. The inner part of Fig. 3 shows the cutoff frequency of the optical frequency response as a function of W_{qw}. This figure implies the increment of cutoff frequency due to widening the QW. It shows that, it is possible to reach 25 GHz bandwidth with QW width of 300 Å. Our previous works show that although wider QW will result in improving the optical frequency response, the current gain of TL (β) will decrease in this manner, because widening the QW increase the probability of recombination in QW, and decrease the carriers who reach the collector, respectively

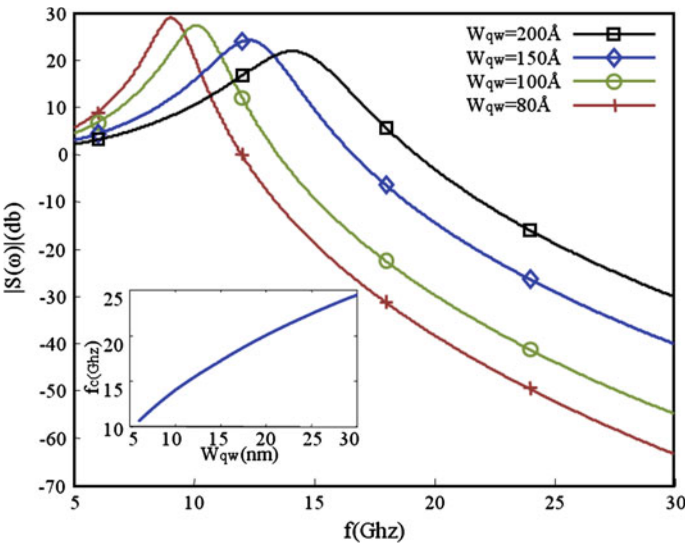

Fig. 3 Main panel: optical frequency response of the TL for different QW widths. Its improvement due to QW width increment is obvious. The inset figure shows the cutoff frequency of TL versus W_{qw}

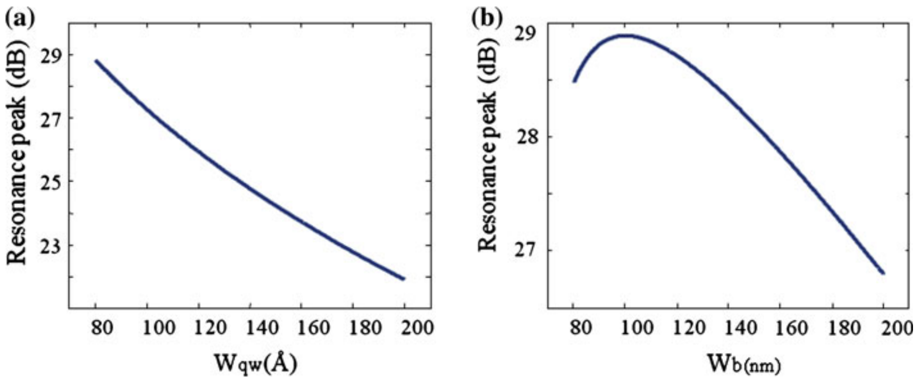

Fig. 4 (**a**) Resonance peak as a function of W_{qw}. This curve shows the decreasing of resonance peak with increasing of W_{qw}. (**b**) Resonance peak as a function of W_b

(Kaatuzian et al. 2011). Figure 4a shows the resonance peak variation as a function of W_{qw} in a more obvious manner. In this figure, it is clear that, 120 Å increment in QW width will result in 8 dB decreasing in resonance peak.

In addition to QW width, the base width of this long wavelength TL, can affect the optical frequency response too. Figure 4b shows the resonance peak versus W_b. It can be seen that the curve has a maximum at 100 nm, near the value, in which Huang et al. fabricated the TL. On the other hand Fig. 5 shows that the TL would have the largest bandwidth with this W_b. This figure shows that for various QW widths, 105 nm is optimum value for W_b, in order to have the largest bandwidth. So unlike QW width, in which lower resonance peak leads to larger bandwidth, there is a tradeoff between bandwidth and resonance peak for base width effect. Finally it should be mentioned that, as it can be seen in Fig. 4, widening the QW

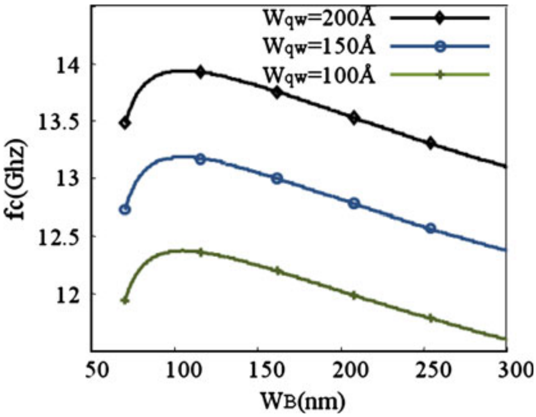

Fig. 5 Cutoff frequency of TL versus base width for different QW widths. The figure shows that there is an optimum value for base width in order to maximizing the bandwidth

reduces the resonance peak about 7 dB but changing W_b will affect the resonance peak only about 2 dB. Similarly the comparison of the inset of Fig. 3 and Fig. 5 shows the larger effect of W_{qw} on the cutoff frequency of TL than W_b. These facts show that W_{qw} has greater effect on optical frequency reponse of TLs than W_b. This is because of the large effect of W_{qw} on probability of carrier capturing in the QW. Although W_{qw} has greater effect on optical frequency response than W_b, since widening the QW reduces the current gain, this parameter cannot be changed widely.

5 Conclusion

In this paper, we have employed charge control model for analyzing the frequency response of a long wavelength HBTL for the first time. In order to achieve this goal, three coupled rate equations for electron and photons have been solved in the base region which includes a single QW. All parameters of the mentioned model have been calculated for this new type of long wavelength TL. The results have shown that, the fabricated HBTL possess a 29 dB resonance peak which is not very desirable. We have analyzed the effect of changing the base width and QW width on optical frequency response and specifically the resonance peak. Although, wider QW will result in less current gain (β), results show that it can decrease the resonance peak and increase the optical bandwidth significantly. 120 Å increment in QW width will result in 8 dB decrease in resonance peak and 15 GHz increase in optical bandwidth.

It is possible to find an optimum value for base width in order to maximize the bandwidth, totally similar to traditional GaAs TLs. Our analysis shows that this value is approximately 1,050 Å for this TL. Unfortunately, it should be noticed that for this base width value, the resonance peak will be maximized too. There are other methods to improve the TL frequency response more including optimization of other parameters of TLs, like base doping, and using more accurate model.

References

Asada, M.: Gain and intervalence band absorption in QW lasers. IEEE J. Quantum Electron. **20**(7), 745–753 (1984)

Berger, V.: Three-level laser based on intersubband transitions in asymmetric quantum wells: a theoretical study. Semicond. Sci. Technol. **9**, 1493–1499 (1994)
Coldren, L.A., Corzine, S.W.: Diode Lasers and Photonic Integrated Circuits. Wiley, New York (1995)
Dixon, F., Feng, M., Holonyak, N., Huang, Y., Zhang, Z.B., Ryou, J.H., Dupuis, R.D.: Transistor laser with emission wavelength at 1544 nm. Appl. Phys. Lett. **93**(2), 021111-1–021111-3 (2008)
Faraji, B., Wei, S., Pulfrey, D.L., Chrostowski, L.: Analytical modeling of the transistor laser. IEEE J. Quantum Electron. **15**, 594–603 (2009). doi:10.1109/JSTQE.2009.2013178
Feng, M., Holonyak, N., Walter, G., Chan, R.: Room temperature continuous wave operation of a heterojunction bipolar transistor laser. Appl. Phys. Lett. **87**, 131103 (2005). doi:10.1063/1.2058213
Feng, M., Holonyak, N., James, A., Cimino, K., Walter, G., Chan, R.: Carrier lifetime and modulation bandwidth of a quantum well AlGaAs/InGaP/GaAs/InGaAs transistor laser. Appl. Phys. Lett. **89**, 113504–113507 (2006). doi:10.1063/1.2346369
Feng, M., Holonyak, N., Then, H.W., Walter, G.: Charge control analysis of transistor laser operation. Appl. Phys. Lett. **91**, 053501–053503 (2007). doi:10.1063/1.2767172
Harrison, P.: Quantum Wells, Wires and Dots. Wiley, New York (2005)
Holonyak, N., Feng, M.: The transistor laser. IEEE Spectr. **43**(2), 50–55 (2006)
Huang, Y., Ryou, J., Dupuis, R.D.: Epitaxial structure design of a long-wavelength InAlGaAs/InP transistor laser. IEEE J. Quantum Electron. **47**(5), 642–650 (2011). doi:10.1109/JQE.2011.2108636
Huang, Y., Ryou, J., Dupuis, R.D., Dixon, F., Holonyak, N., Feng, M.: InP/InAlGaAs light-emitting transistors and transistor lasers with a carbon-doped base layer. J. Appl. Phys. **109**, 063106–063112 (2011). doi:10.1063/1.3561368
Kaatuzian, H.: Photonics, vol. 1. pp. 193 Amirkabir University of Technology Press, Tehran (2005)
Kaatuzian, H., Rahbardar, H., Taghavi, I.: Optical modulation bandwidth enhancement of heterojunction bipolar transistor lasers using base width variation. In: NUSOD 2011 proceeding (2011)
Smet, J.H., Fonstad, C.G., Hu, Q.: Intrawell and interwell intersubband transitions in multiple quantum wells for far-infrared sources. J. Appl. Phys. **79**, 9305–9320 (1996). doi:10.1063/1.362607
Taghavi, I., Kaatuzian, H.: Gain-bandwidth trade-off in a transistor laser: quantum well dislocation effect. Opt. Quant. Electron. **41**, 481–488 (2010). doi:10.1007/s11082-010-9384-0
Then, H.W., Feng, M., Holonyak, N., Wu, C.H.: Experimental determination of the effective minority carrier lifetime in the operation of a quantum-well n-p-n heterojunction bipolar light-emitting transistor of varying base quantum-well design and doping. Appl. Phys. Lett. **91**, 033505–033508 (2007). doi:10.1063/1.2759263
Zhang, L., Leburton, J.P.: Modeling of the transient characteristics of heterojunction bipolar transistor lasers. J. Appl. Phys. **45**, 359–366 (2009). doi:10.1109/JQE.2009.2013215